

RSC Advances



This is an *Accepted Manuscript*, which has been through the Royal Society of Chemistry peer review process and has been accepted for publication.

Accepted Manuscripts are published online shortly after acceptance, before technical editing, formatting and proof reading. Using this free service, authors can make their results available to the community, in citable form, before we publish the edited article. This *Accepted Manuscript* will be replaced by the edited, formatted and paginated article as soon as this is available.

You can find more information about *Accepted Manuscripts* in the [Information for Authors](#).

Please note that technical editing may introduce minor changes to the text and/or graphics, which may alter content. The journal's standard [Terms & Conditions](#) and the [Ethical guidelines](#) still apply. In no event shall the Royal Society of Chemistry be held responsible for any errors or omissions in this *Accepted Manuscript* or any consequences arising from the use of any information it contains.

Mechanical properties and variation SOC going from La to Nd in intermetallics RIn_3 and RSn_3 (R= La, Ce, Pr, Nd)

M. Shafiq^{1,2}, Iftikhar Ahmad^{1,2*}, S. Jalali-Asadabadi^{3**}

1. Center for Computational Materials Science, University of Malakand, Pakistan
2. Department of Physics, University of Malakand, Chakdara, Pakistan
3. Department of Physics, Faculty of Science, University of Isfahan, Hezar Gerib Avenue, Isfahan 81744, Iran

* Corresponding author: Iftikhar Ahmad Ph.D. (Idaho, USA)
Center for Computational Materials Science
University of Malakand, Chakdara, Pakistan
ahma5532@gmail.com (092)332-906-7866

** Corresponding author: Saeid Jalali-Asadabadi, Ph.D. (IUT, Iran)
Department of Physics, Faculty of Science,
University of Isfahan (UI), HezarGerib Avenue,
Isfahan 81746-73441, Iran
saeid.jalali.asadabadi@gmail.com, sjalali@sci.ui.ac.ir
(+989133287908)

ABSTRACT

First principle studies of the cubic rare-earth intermetallics RIn_3 and RSn_3 (R= La, Ce, Pr, Nd) have been carried out within the framework of density functional theory using the full potential linearized augmented plane waves plus local orbital method (FP-LAPW+lo). The calculated structural parameters with different exchange correlation functional are found consistent with the experimental results. The effect of Hubbard potential on the density of states is discussed in details. It is observed that the inclusion of spin-orbit coupling (SOC) causes degeneracies of the electronic band structure in the vicinity of the Fermi level of these compounds. Furthermore, the SOC effect enhances as one goes from La to Nd in a compound, which demonstrates interesting nature of this effect in periodic table. The elastic constants, bulk moduli, shear moduli, Young's moduli, anisotropy, Kleinman parameters, Poisson's ratios, sound velocities for shear and longitudinal waves, and Debye temperatures are calculated and discussed, which reveal that these compounds are ductile in nature.

Key Words: Rare-earth intermetallics; strongly correlated electron systems; mechanical properties; spin-orbit coupling; ab-initio calculations

I. INTRODUCTION

The rare-earth (RE) intermetallic compounds are strongly correlated electron systems, where in this family of compounds RX_3 (R = rare-earth and X =In, Sn) are most exciting for their interesting physics. The RX_3 compounds have attracted both experimental and theoretical attentions because of their diverse bulk properties such as low superconducting transition temperature, magnetic susceptibility and thermoelectric power as a function of their electron concentration.^{1, 2} These compounds offer many possibilities by replacing X atom (X =In, Sn, Tl, Pb, etc), and their single crystals can be easily grown due to their congruently melting.³ Many of the RX_3 compounds crystallize in the cubic symmetries which is more favorable structure for superconductivity than lower symmetry.⁴ Furthermore, these compounds are stable in the cubic structure at standard temperature and pressure (STP) and remain stable over a wide range of pressures.⁵ In RSn_3 solders (Sn-solder) the rare-earth element La, Ce, Er and Eu are used which is a suitable replacement of the Pb-Sn solder.⁶ The amount of RE element in Sn-solder improves both the physical and mechanical properties and particularly enhances the ductility of the solder.⁷

Due to the unfilled 4f orbitals and spin-orbit interactions the adjacent electronic states strongly interact with each other, therefore the characterization of accurate physical properties and the development of analytical and computational tools for the lanthanide based compounds is a challenging problem for both, experimental and theoretical researchers.⁸ RX_3 (R = La, Ce, Pr and Nd, X = In and Sn) intermetallic compounds crystallize in the cubic $AuCu_3$ -type crystal structure with space group $Pm-3m$ (No. 221). The point groups of R and X atoms are the cubic $m-3m$ and non-cubic $4/mmm$, respectively.⁹ In the RX_3 compounds, the valency of lanthanide can be inferred through lattice constant measurement technique. The lattice constant of R^{2+} is larger than R^{3+} by almost 10% for pure lanthanides.¹⁰ For diluted lanthanides RX_3 (R = Eu, Yb)

(addition of other elements with lanthanides), the lattice constant increases less than 2% as compared to other LnX_3 compounds. This shows unusual nature of Eu and Yb, which display divalency in these $4f$ series of compounds.^{9,11} Most of RIn_3 and RSn_3 compounds are antiferromagnetic (AFM)^{12,13} except Pauli paramagnetic LaIn_3 , and paramagnetic LaSn_3 , CeSn_3 and PrIn_3 .¹⁴⁻¹⁶ The AFM transition Néel temperature (T_N) for CeIn_3 , NdIn_3 , PrSn_3 and NdSn_3 are 10 K, 5.9 K, 8.6 K, and 4.7 K respectively.¹⁷⁻¹⁹ Some of RIn_3 and RSn_3 exhibit superconductivity. The superconducting transition temperatures (T_C) for LaIn_3 , LaSn_3 and CeIn_3 are 0.71 K, 6.5 K, and 0.2 K, respectively.^{20,21} Moreover CeIn_3 and PrSn_3 are heavy fermions compounds.^{22,23} Due to both localized and itinerant characters of f electrons CeIn_3 is also called mixed valence or intermediate valence²⁴ and CeSn_3 is categorized as Kondo compound with valence fluctuation.²⁵ The Fermi surface properties and de Haas–van Alphen (dHvA) effect in RX_3 compounds are reported by Onuki and Settai²⁶, whereas the pressure dependent electronic structure and optical conductivity of CeIn_3 compound in AFM phase are experimentally investigated by Iizuka et al.²⁷

Some theoretical studies on the pressure dependent structural, electronic and elastic properties of the intermetallic compounds LaIn_3 , LaSn_3 , CeIn_3 and CeSn_3 are available^{1,2,28,29} in literature but their theoretical results are not consistent with the experiments because of the improper treatment of the exchange correlation potential in those calculations. In these studies, they have used local density approximation (LDA) and generalized gradient approximation (GGA); where it is evident that RIn_3 and RSn_3 compounds are strongly correlated electron systems with $4f$ electrons. Therefore, to obtain the rational and logical electronic structure and other physical properties of these compounds, it is necessary to treat the strong correlation effects by an additional local Hubbard repulsion of magnitude U , i.e., DFT+ U techniques as well

as spin-orbit coupling (SOC) effect to increase the accuracy of the calculated results. These deliberations are considered in carrying out the calculations of the structural, electronic, elastic and mechanical properties of the intermetallic compounds, RX_3 ($R = \text{La, Ce, Pr and Nd}$, $X = \text{In and Sn}$). The calculations are carried out by using the full potential linearized augmented plane waves plus local orbitals (FP-LAPW+lo) method under the frame work of DFT. We have carried out these studies with the motivation that the elastic and mechanical properties of CeIn_3 , CeSn_3 , PrIn_3 , PrSn_3 , NdIn_3 and NdSn_3 have never been explored, neither theoretically nor experimentally, which may have promising materials with improved mechanical properties for practical applications. This study will cover the missing information in literature about these materials and will also provided basis for future experiments.

II. METHOD OF CALCULATIONS

The calculations have been performed by using the density functional theory (DFT) implemented in the WIEN2k code³⁰ and employing the full potential linearized augmented plane waves plus local orbitals (FP-LAPW+lo) method.³¹ The exchange correlation effects are calculated within the local density approximation (LDA)³², generalized gradient approximation (GGA)³³, GGAsol³⁴, Wu–Cohen GGA (WC-GGA)³⁵, meta GGA (m-GGA)³⁶ and hybrid functional B3PW91^{37,38} with spin polarization. As lanthanides are strongly correlated systems with localized $4f$ electrons,^{39,40} therefore to obtain the exact nature of the electronic structure of the compounds under consideration, we use LDA+U and GGA+U methods. The DFT+U method is based on the Hubbard model, which treats the strongly correlated electron systems with an orbital dependent potential of Coulomb and exchange interaction.⁴¹ The optimized values of the U parameter are obtained by varying U, step by step. After examining several values of U

parameter and selected the values which give better result of magnetic moment compared to the experimental value for the corresponding compounds. The values of U used within the calculations are given in Table 1. One can clearly see a trend of increasing U with increasing atomic number. This is because that with increasing atomic number, the *f* state becomes deeper and the orbitals become more localized, thus leading to an increased Coulomb interaction. Furthermore, spin-orbit coupling (SOC) is included to treat the relativistic effects. The SOC are included by a second variational method.⁴² The second variational method, which makes use of the scalar-relativistic basis, based on the reduction of the original basis. In the first step of this approach, the scalar-relativistic part of the Hamiltonian is diagonalized in the scalar-relativistic basis. In the second step the full Hamiltonian matrix including SOC is constructed using the eigen functions of the first step Hamiltonian. Once the effects of the spin-orbit coupling are included, then the full Hamiltonian can be written as:

$$H\tilde{\psi} = \varepsilon\tilde{\psi} + H_{so}\tilde{\psi} \quad (1)$$

where, H_{so} is spin-orbit Hamiltonian and is given by:⁴³

$$H_{so} = \frac{\hbar}{2Mc^2} \frac{1}{r} \frac{dV}{dr} \begin{pmatrix} \vec{\sigma} \cdot \vec{l} & 0 \\ 0 & 0 \end{pmatrix} \quad (2)$$

With $\vec{\sigma}$ is Pauli spin matrices.

The radii of the muffin-tin sphere have been chosen as 2.50 a. u. for the rare-earth elements as well as for Sn and In. To achieve convergence the basis set is expanded in terms of plane waves up to $R_{MT} K_{max} = 7$ where R_{MT} is the smallest atomic radius in a unit cell and K_{max} is the magnitude of the maximum value of k-vector in the plane waves expansion. For the valence wave function inside a muffin-tin spheres the maximum value of angular momentum $l_{MAX} = 10$ is considered. In the interstitial region the charge density is Fourier expanded up to $G_{max} = 12$. As

high accuracy is required to calculate elastic properties, therefore by increasing the number of k-points we tested the convergence of the total energy and hence the total energy is converged for 6000 k-points with a dense k mesh of 165 k-points in the irreducible wedge of the Brillouin zone having grid size of $18 \times 18 \times 18$ using the Monkhorst and Pack mesh.⁴⁴

The elastic constants of RX_3 are calculated with the Cubic-elastic software,⁴⁵ using the energy approach⁴⁶ implemented in the WIEN2k code. In this work Voigt notations are replaced, which decreases the number of elastic constants and hence for cubic lattice only three independent elastic constants C_{11} , C_{12} and C_{44} are left, which can be determined by introducing orthorhombic, cubic and monoclinic lattice distortions.⁴⁷ These constants are calculated, which are further used to evaluate the mechanical properties of RX_3 such as shear modulus (G), Young's modulus (Y), Cauchy pressure (C''), Poisson ratio (ν), Kleinman parameter (ξ), and anisotropy constant (A) by using standard relations.^{47,48}

TABLE 1. Values of U and used for the RIn_3 and RSn_3 .

Comp.	$LaIn_3$	$LaIn_3$	$LaIn_3$	$LaIn_3$	$LaSn_3$	$LaSn_3$	$LaSn_3$	$LaSn_3$
U (eV)	5.0	5.5	5.8	6.2	5.0	5.5	5.8	6.2

III. RESULTS AND DISCUSSIONS

A. Ground state structural properties

The ground state structural properties of RX_3 ($R = La, Ce, Pr$ and Nd , $X = In$ and Sn) are calculated by finding the total energy of the unit cell for each compound with respect to volume using Birch–Murnaghan equation of state.⁴⁹ Lattice constant (a) and zero pressure bulk moduli

(B_0) are determined by a variety of schemes including, LDA, GGA, GGAsol and WC-GGA, LDA+U, and GGA+U as well as m-GGA and B3PW91 hybrid functional.

The theoretically calculated results of lattice constants and bulk moduli along with the available experimental data are listed in Table 2 and 3, respectively.

The calculated GGA, GGA+U and m-GGA lattice constants are slightly larger than those of GGA-sol, WC-GGA, LDA+U and B3PW91, while the calculated values for the bulk moduli by GGA, GGA+U and m-GGA for these compounds are smaller than those of the GGA-sol and WC-GGA and B3PW91. This confirms that the general trend of these approximations, GGA overestimates and LDA underestimates lattice constants.³⁴ The Table 2 indicates that the computed lattice constants with B3PW91 hybrid functional are in better agreement with the experimental values than the other theoretical approaches. It is further clear from the table that B3PW91 is the best performing functional for strongly correlated systems as compared to the other schemes. Table 2 also shows that as we move from La to Nd, the lattice constants are contracted, which can be attributed to the lanthanide contraction, i.e., the decrease in the atomic radius along the lanthanide series from left to right due to the poor shielding effect of the 4f electrons. Table 3 shows that the calculated bulk moduli by B3PW91 for all the compounds are very close to each other and lie in the range of 52.950 and 70.686 GPa. This trend of the bulk moduli is also evident from the calculated results by GGA-sol, GGA, m-GGA WC-GGA and LDA+U. No experimental data to the best of our knowledge is available for the bulk moduli, so our results are considered as a prediction for these properties of RIn_3 and RSn_3 (R=La, Ce, Pr and Nd) compounds.

TABLE 2. The calculated value of lattice parameters (a in Å) of RIn_3 and RSn_3 ($R=La, Ce, Pr$ and Nd) compounds.

Comp.	LDA	GGA _{sol}	GGA	WC	LDA+U	GGA+U	B3PW91	m-GGA	Exp.
$LaIn_3$	4.645	4.697	4.787	4.704	4.698	4.835	4.738	4.789	4.732 ^a
$CeIn_3$	4.554	4.601	4.718	4.609	4.612	4.761	4.676	4.708	4.687 ^a
$PrIn_3$	4.546	4.605	4.705	4.617	4.647	4.795	4.669	4.701	4.670 ^a
$NdIn_3$	4.540	4.603	4.689	4.609	4.626	4.765	4.647	4.696	4.653 ^a
$LaSn_3$	4.686	4.728	4.816	4.736	4.738	4.864	4.773	4.815	4.769 ^b
$CeSn_3$	4.589	4.626	4.755	4.637	4.636	4.785	4.710	4.749	4.721 ^b
$PrSn_3$	4.582	4.632	4.729	4.647	4.661	4.839	4.709	4.734	4.716 ^b
$NdSn_3$	4.581	4.624	4.713	4.637	4.644	4.776	4.701	4.713	4.705 ^b

^aReference 13.

^bReference 66.

TABLE 3. The calculated value of bulk moduli (B_0 in GPa) of RIn_3 and RSn_3 ($R=La, Ce, Pr$ and Nd) compounds.

Comp.	LDA	GGA _{sol}	GGA	WC	LDA+U	GGA+U	B3PW91	m-GGA
$LaIn_3$	60.816	58.184	52.293	58.653	60.188	53.720	56.213	52.157
$CeIn_3$	74.382	63.580	52.703	63.166	61.029	51.628	61.100	50.536
$PrIn_3$	63.110	61.015	53.319	61.106	54.015	59.587	53.044	54.791
$NdIn_3$	63.493	61.943	52.527	59.278	69.926	49.240	64.591	49.120
$LaSn_3$	65.837	60.339	53.861	59.064	61.507	56.910	55.646	50.004
$CeSn_3$	79.210	71.621	67.212	71.920	71.445	55.026	70.686	60.948
$PrSn_3$	70.565	66.817	52.580	64.541	67.438	52.322	55.720	49.704
$NdSn_3$	72.514	62.381	56.295	66.712	69.969	51.222	52.950	51.046

B. Electronic Structure and Density of States

In order to reveal the electronic band structure, spin polarized total density of states (TDOS) and $4f$ density of states are calculated by employing GGA and LDA for the exchange and correlation functional. The DOSs calculated by GGA and LDA approximations are quite similar and only GGA density of states and $4f$ -DOS for RIn_3 and RSn_3 ($R=La, Ce, Pr$ and $Nd, X=In$ and Sn) are

presented in Fig. 1, where the Fermi level is set at 0 eV. It is clear from the figure that no band gap is available at Fermi level for any of the intermetallic compounds under consideration; hence all these compounds are metallic in nature. The figure also reveals the dominating character of the f state in all these compounds. It is also evident from the figure that no prominent peak occurs at the Fermi level for any of these compounds under study; therefore all these compounds are ductile in nature. The maximum peak of LaIn_3 and LaSn_3 are above the Fermi level in the unoccupied states around 2.74 eV and 2.95 eV, respectively. Therefore, LaIn_3 and LaSn_3 compounds show more ductility than the remaining RIn_3 and RSn_3 compounds, which is due to the large separation between the Fermi level and the f states according to previous study.⁵⁰ The strongly correlated systems such as lanthanides (actinides)^{39,51} which involve $4f$ ($5f$) orbitals have interesting physical and chemical properties, because these electrons can be localized or itinerant depending on the crystalline environment. Therefore, to understand the effects of the $4f$ orbitals in these compounds, the calculations are also carried out with the Hubbard potential U (GGA+ U and LDA+ U). The total density of states (TDOS) with GGA+ U and partial density of

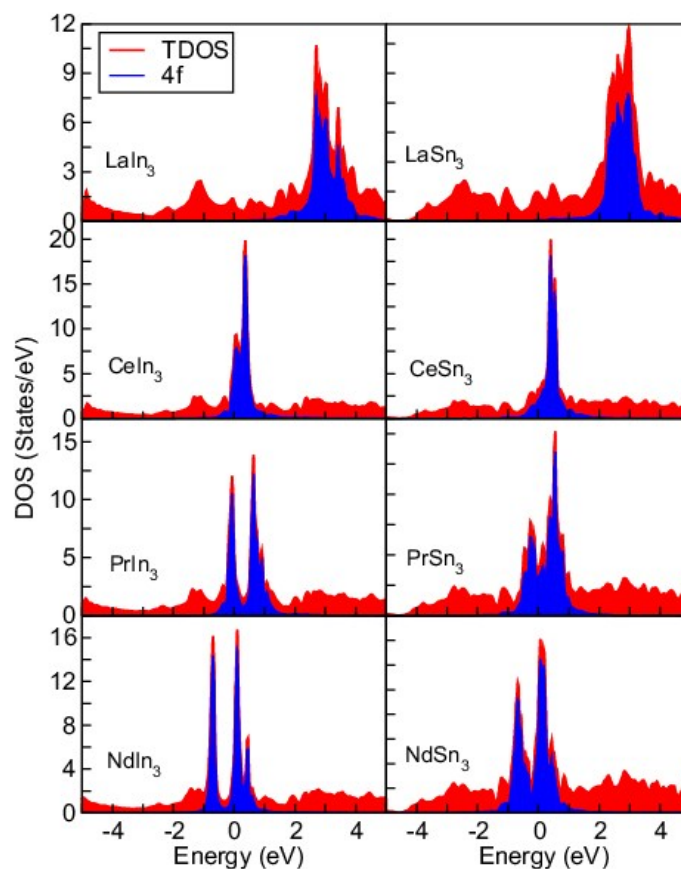


FIG. 1. (Colors online): Total density of states TDOS (red shading) and partial 4f DOS (Blue Shading) of RIn₃ and RSn₃ for R= La, Ce, Pr and Nd calculated with GGA

states (DOS) of *f* states, as well as, the TDOS with- GGA are plotted in Fig. 2. It is clear from the figure that both GGA and GGA+U provides different DOS. The differences in the DOSs for all the compounds can be clearly seen from the figure. The figure clearly indicates that the strong peaks which are due to the 4*f* states are significantly shifted up and down by the application of the Hubbard potential (*U*) as compared to the GGA scheme. This is in agreement with the previous DFT calculations that Hubbard potential opens the gap between the occupied and unoccupied states.⁵²

Spin-orbit coupling (SOC), which was apparently a weak relativistic correction to the Schrödinger equation in condensed matter physics has recently attracted enormous attention in the modern condensed-matter physics because of its key role in 5d, 4f and 5f electronic states. The spin and orbital degrees of freedom are entangled at a local level by the SOC, where the total angular momentum provides a good description of the ordered phases and fluctuation properties of a material and can also describe the possible uses of a material in various devices with prominent functionalities.⁵³ To see the effect of the spin-orbit coupling (SOC) in the compounds under study their band structures along high symmetry directions with GGA and GGA+SO are presented in Fig. 3. It is clear from the figure that the effect on the band structures

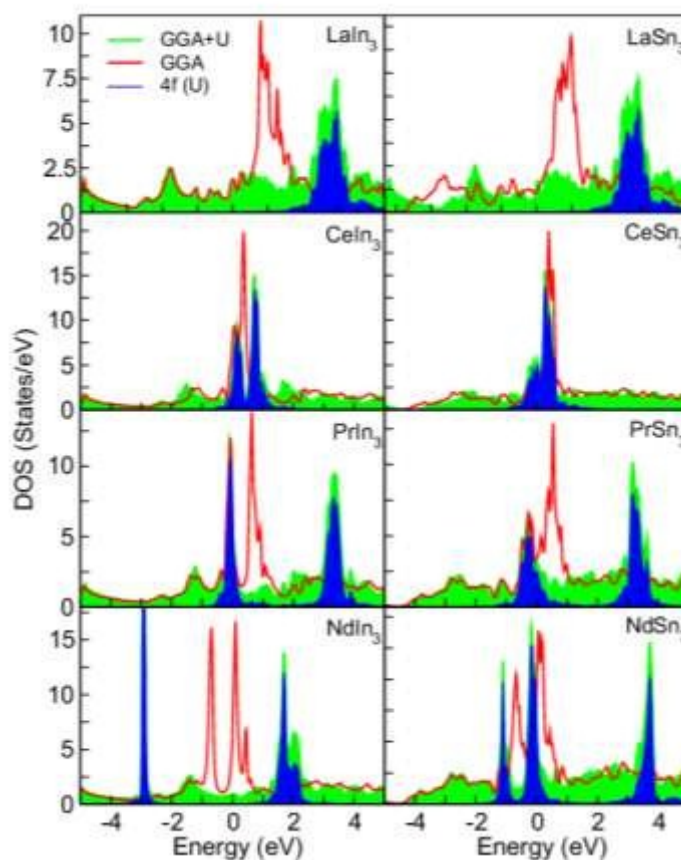


FIG. 2. (Colors online): Total density of states (TDOS) with GGA (red lines), GGA+U (green shading) and PDOS GGA+U-4f of RIn_3 and RSn_3 for $R = La, Ce, Pr$ and Nd .

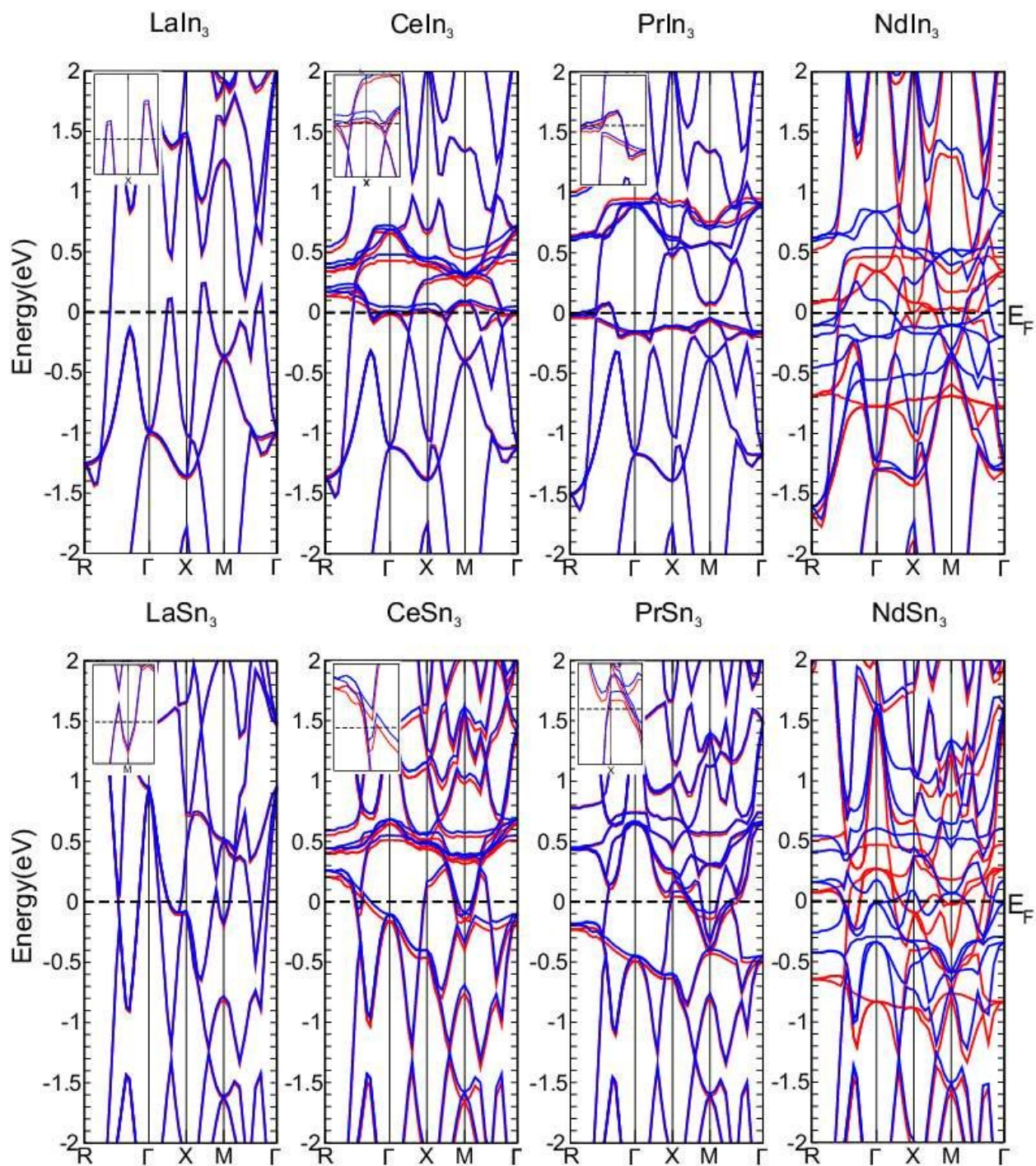


FIG. 3. (Colors online): Comparison of electronic band structures calculated with GGA and SOC for RIn_3 and RSn_3 . The red lines show band structure with GGA without SOC, while the blue lines show the band structure with SOC.

of LaIn_3 and LaSn_3 is very small, which is in agreement with the earlier work.^{1,54} The comparison of the band structures of these compounds reveals that, as one moves from La to Nd, the effect of SOC increases. This might be due to the fact that as the Coulomb attraction on an electron in a particular orbit increases, from La to Nd in the Periodic Table, the orbit shrinks and hence the electron speeds up to conserve the momentum of the system; where with this increase in the speed the relativistic effects of SOC increases. The differences between the GGA and GGA+SOC band structures at the vicinity of the Fermi level are shown in the inset of each compound in Fig. 3 lifting some degeneracies in the band structures. The figure also shows that the band along symmetry line between X and M in CeIn_3 compound, dips below the Fermi level in the GGA scheme but stays above the Fermi level when the SOC is introduced. The degeneracy in PrIn_3 is observed at R symmetry line, whereas in CeSn_3 and PrSn_3 the degeneracies occur at M symmetry line. The SOC effects can be clearly seen for different symmetry lines in NdIn_3 and NdSn_3 .

C. Elastic and Mechanical Properties

The elastic constants of solids provide significant information about the nature of the forces operating in solids. Elastic constants are very important for understanding the relation between the crystal structure and bonding nature. These constants also reveal the structural stability and various other important physical properties of materials. The elastic constants C_{11} , C_{12} , and C_{44} for RIn_3 and RSn_3 (R= La, Ce, Pr and Nd) are calculated within GGA and GGAsol with spin polarization and are given in Table 4. The available experimental elastic constants (for LaSn_3) along with other theoretical results are also listed in the table. No experimental data is available for these compounds except LaSn_3 . It is clear from the table that our calculated values for the

elastic constants of LaSn_3 compound with GGAsol are in excellent agreement with the experimental results of Stassis *et al.*⁵⁵, extracted from the phonon dispersion curves, as compared to other theoretical results reported in Refs. [1, 28]. Hence, from the consistency of our calculated values with the experimental results for this compound, we infer that our calculated values for the remaining compounds under investigation will be also consistent with the corresponding experimental values. Moreover, the stability criteria initiated by Born⁵⁶ for cubic systems in term of elastic constants, i.e., $C_{11}-C_{12} > 0$, $C_{44} > 0$ and $C_{11}+2C_{12} > 0$ are well satisfied by these compounds. The fulfillment of these criteria justifies that these intermetallic compounds are elastically stable.

The trend of the mechanical properties of a material could be estimated from its elastic constants. As the elastic constants C_{11} , C_{12} , and C_{44} , calculated by both, GGA and GGAsol, exchange and correlation effects are very close to each other; therefore in this article the mechanical properties of the compounds are evaluated by the GGAsol results. The main mechanical parameters, i.e. shear modulus (G), Young's modulus (Y), Pugh's ratio (B/G), Cauchy's pressure (C''), Poisson's ratio (ν) and anisotropic ratio (A), which are important for industrial applications are calculated and presented in Tables 5. These important parameters are used to characterize the mechanical behavior of a material.

The average Hill's⁵⁷ shear modulus, $G_H = G$, as a measure resistance to plastic deformations upon shear stress is the arithmetic mean of Reuss and Voigt shear modulus.^{58,59} The value of G_H given in Table 5 indicates that CeSn_3 offers more resistance to plastic deformation than the remaining compounds. The Young's modulus (Y) defines the ratio between the linear stress and strain. The larger the value of Y , the stiffer will be the material. From Table 5 one can see that CeSn_3 has larger value of Young's modulus (stiffer). The higher values for

the Young's moduli as compared to their Bulk moduli confirm the stiffness of these compounds. Hill's and shear moduli are further used to explain the ductile and brittle nature of a compound.

TABLE 4. The calculated values of elastic constants C_{11} , C_{12} , C_{44} (GPa) with GGAsol and (GGA).

Comp.	E_{XC}	LaIn ₃	CeIn ₃	PrIn ₃	NdIn ₃	LaSn ₃	CeSn ₃	PrSn ₃	NdSn ₃
C_{11}	GGAsol	89.265	95.500	83.878	82.569	69.273	99.084	80.343	87.167
	GGA	97.525	100.909	80.152	85.405	86.732	85.005	80.247	96.191
	Exp. others					70.50 ^a 97.30 ^b , 83.17 ^c			
C_{12}	GGAsol	42.555	45.609	37.137	41.498	42.328	53.678	38.842	34.211
	GGA	50.885	49.383	29.183	60.287	43.855	57.967	44.094	25.357
	Exp. other					42.00 ^a 53.6 ^b , 45.51 ^c			
C_{44}	GGAsol	27.280	29.879	32.365	35.340	27.584	48.904	28.575	30.375
	GGA	28.125	37.543	34.767	33.997	35.463	45.431	28.370	27.367
	Exp. other					33.50 ^a 44.20 ^b , 31.22 ^c			

^aReference 55.

^bReference 1.

^cReference 28.

Pugh⁶⁰ suggested index of ductility and brittleness of a material. The Pugh's ratio (B/G) reflects the competition between the shear and cohesive strength of a material and describes its ductile/brittle character. If B/G is greater than the critical value 1.75, the material behaves in a ductile manner; otherwise the material will be brittle in nature. It is evident from Table 5, that B/G ratio for all RIn₃ and RSn₃ compounds show ductile behavior ($B/G > 1.75$). The larger value of B/G for LaSn₃ (2.412) and for LaIn₃ (2.267) reveals higher value of ductility. The same nature has also been observed in the DOS plot (fig. 1) for LaSn₃ and LaIn₃, showing more ductile nature than the other compounds. Ductile and brittle behavior of a compound can be also discussed in

terms of elastic constants C_{12} and C_{44} . The Cauchy's pressure ($C'' = C_{12} - C_{44}$) is used for this purpose and its positive/negative value shows the ductile/brittle behavior of a compound. The positive value of Cauchy's pressure (from table 5) indicates that all the compounds under investigation are ductile in nature, which confirms the results of Pugh's B/G ratio. The Cauchy's pressure is also used to indicate the bonding character of the compounds. The positive value of Cauchy pressure is responsible for ionic bonding, while a material with negative Cauchy pressure requires angular or directional character in bonding (covalent bonding). It is clear from Table 5 that all the compounds possess positive value of Cauchy's pressure having metallic bond and hence high mobility characteristics.

Poisson's ratio ν usually quantifies the stability of a crystal against shear (compressibility). Its typical lower and upper bound limits are -1 and 0.5 respectively. The lower limit bound is where the material does not change its shape and the upper limit bound is where the volume remains unchanged.⁶¹ Our calculated values for Poisson's ratio lie between 0.313 and 0.265, which show that these materials are less compressible and stable against external deformation. Poisson's ratio also demonstrates the ductile/brittle nature of a material. For ductile compounds $\nu \approx 0.3$ and for brittle $\nu > 0.35$. The Poisson's ratio for all of these compounds is less than 0.35, which further confirms the ductile nature of these compounds. Furthermore, the Poisson's ratio also gives the information about bonding forces. For central forces in solids, the lower limit of ν is 0.25 and upper limit of ν is 0.5.⁶² The table shows that the calculated values of Poisson's ratio fall in this limit and the dominant interatomic forces are central forces. Kleinman internal strain parameter (ζ) describes the relative tendency of bond bending versus bond stretching.⁶³ Minimizing bond bending leads to $\zeta = 0$, while, minimizing bond stretching

leads to $\zeta = 1$. The calculated Kleinman parameters in Table 5 predict that in RIn_3 and RSn_3 compounds bond stretching is dominant (upper limit of ζ).

Anisotropic ratio (A) which measures the elastic anisotropy of a material is very important property and is closely related to the induced microcracks in a material.⁶⁴ For an ideal isotropic material, anisotropic ratio is unity and deviation from unity measures the amount of anisotropy. From Table 5 one can see that the value of anisotropic ratio is found to be much greater than 1. The deviations from unity specify that these compounds are not elastically isotropic and their properties strongly vary in different directions.

TABLE 5. The calculated values of Voigt's shear modulus G_V , Reuss's shear modulus G_R , Hill's shear modulus G_H , B/G ratio, Cauchy Pressure (C''), Poisson's ratio (ν), Kleinman Parameter (ζ), Anisotropy constant (A), and Shear Constant (C').

Comp.	$LaIn_3$	$CeIn_3$	$PrIn_3$	$NdIn_3$	$LaSn_3$	$CeSn_3$	$PrSn_3$	$NdSn_3$
G_V	25.710	27.906	28.767	29.418	22.139	38.424	25.445	28.816
G_R	25.562	27.689	28.047	27.430	19.849	33.459	24.830	28.686
G_H	25.636	27.797	28.407	28.424	20.994	35.941	25.138	28.916
Y	67.219	72.832	73.020	74.939	57.971	97.183	65.749	72.940
B/G	2.267	2.239	1.856	1.942	2.412	1.915	2.095	1.794
C''	15.275	15.730	4.772	6.158	13.744	4.774	10.267	3.836
ν	0.307	0.305	0.269	0.274	0.309	0.265	0.292	0.266
ζ	0.796	0.797	0.743	0.838	0.994	0.902	0.807	0.666
A	1.168	1.198	1.385	1.721	1.974	2.154	1.377	1.147
C'	23.355	24.946	23.371	20.536	13.973	22.703	20.751	26.478

The important parameter, which defines the dynamical stability of a material, is shear constant C' . It is also one of the criterions of mechanical stability and shows stability to the tetragonal distortion. Its values for the compounds under consideration are given in the Table 5. The positive values of shear constant ($C' > 0$) fulfills the required criteria of dynamical stability.

From the calculated value of C' it is predicted that these compounds are dynamically stable materials.

D. Sound Velocities and Debye Temperature:

The thermo-physical properties like longitudinal v_l , transverse v_s , average sound velocities v_m , and Debye temperature $\theta(D)$ of the compounds under study are also investigated. The Debye temperature $\theta(D)$ of a compound can be calculated by using the following relation:⁶⁵

$$\theta(D) = \frac{h}{k_B} \left[\frac{3n}{4\pi} \left(\frac{N_A \rho}{M} \right) \right]^{\frac{1}{3}} v_m, \quad (2)$$

where h is the Plank's constant and K_B is the Boltzmann's constant, N_A is the Avogadro's number, ρ is density, M is the molecular weight, v_m is the average sound velocity and n is the number of atoms per formula unit. Similarly, the average sound velocity for any compound can be calculated the following equation:

$$v_m = \left[\frac{1}{3} \left(\frac{2}{v_s^3} + \frac{1}{v_l^3} \right) \right]^{-\frac{1}{3}}, \quad (3)$$

where v_l and v_s are the longitudinal and transverse sound velocities which can be obtained in term of shear modulus G and the bulk modulus B_0 as:

$$v_l = \left[\frac{B + \frac{4G}{3}}{\rho} \right]^{\frac{1}{2}}, \quad \text{and} \quad v_s = \left[\frac{G}{\rho} \right]^{\frac{1}{2}}. \quad (4)$$

The calculated theoretical densities, sound velocities and Debye temperatures are reported in Table 6. The calculated densities are in excellent agreement with available experimental value in parentheses. A material with greater Debye temperature will be stiffer and exhibits high thermal

conductivity. Table 6 shows that CeSn₃ is stiffer than the other compounds ($\theta(D)=151.05$), which confirms the result of Young's modulus for CeSn₃ ($Y= 97.183$). The lower Debye temperature of LaSn₃ is the consequences of lower elastic constants as compared to the rest of the compounds.

TABLE 6. The calculated values of density ρ (g/cm³), sound velocity of transverse wave v_s (m/s), sound velocity of longitudinal waves v_l (m/s), average velocity v_m (m/s) and Debye temperature $\theta(D)$ (K) of compounds.

Comp.	ρ	v_l	v_s	v_m	$\theta(D)$
LaIn ₃	7.316(7.45 ^a)	3551.97	1871.88	2092.91	130.18
CeIn ₃	7.661	3600.34	1904.86	2166.58	136.73
PrIn ₃	7.737	3421.79	1916.10	2132.72	134.78
NdIn ₃	7.871	3439.08	1900.38	2117.45	134.46
LaSn ₃	7.358(7.46 ^a)	3269.06	1689.14	1891.06	116.92
CeSn ₃	7.664	3902.84	2165.59	2412.16	151.05
PrSn ₃	7.804	3323.42	1794.79	2003.25	126.14
NdSn ₃	7.936	3375.35	1908.81	2122.88	134.12

^aReference 3.

IV. Conclusions:

In summary, we have performed theoretical analysis of the structural, electronic and elastic properties of RIn₃ and RSn₃ (R= La, Ce, Pr and Nd) using density functional theory. The calculated structural properties of the compounds are consistent with the experimental results. The density of states and band structures reveal the intermetallic nature of these compounds. It is concluded that the spin-orbit coupling effect, which is a correction to Schrödinger wave equation, enhances as one goes from La to Nd in a compound, which demonstrates interesting nature of this effect in periodic table. We discussed the influence of the spin-orbit coupling

strength on the band structure. Mechanical properties were also evaluated using elastic constants. From the calculated elastic properties and other mechanical properties, all the compounds investigated are found to be ductile in nature with elastic anisotropy.

References

1. S. Ram, V. Kanchana, G. Vaitheeswaran, A. Svane, S. B. Dugdale and N. E. Christensen, *Phys. Rev. B*, 2012, **85**, 174531.
2. S. Ram, V. Kanchana, A. Svane, S. B. Dugdale and N. E. Christensen, *J. Phys.: Condens. Matter*, 2013, **25**, 155501.
3. R. J. Gambino, N. R. Stemple and A. M. Toxen, *J. Phys. Chem. Solids*, 1968, **29**, 295.
4. I. R. Harris and G. V. Raynor, *J. Less-Common Metals*, 1965, **9**, 7.
5. N. V. C. Shekar and P. C. Sahu, *J. Mater. Sci.*, 2006, **41**, 3207.
6. C. F. Li, Z. Q. Liu, P. J. Shang and J. K. Shang, *Scr. Mater.*, 2011, **65**, 1049.
7. M. A. Dudek and N. Chawla, *Intermetallics*, 2010, **18**, 1016.
8. I. N. Yakovkin, T. Komesu and P. A. Dowben, *Phys. Rev. B*, 2002, **66**, 035406.
9. S. J. Asadabadi, S. Cottenier, H. Akbarzadeh, R. Saki and M. Rots, *Phys. Rev. B*, 2002, **66**, 195103.
10. K. A. Jr. Gschneider, *Solid State Phys.*, 1964, **16**, 275.
11. S. Jalali Asadabadi and H. Akbarzadeh, *Physica B*, 2004, **349**, 76.
12. Z. Kletowski, *Solid State Commun.*, 1989, **72**, 901.
13. K. H. J. Buschow, H. W. de Wijn and A. M. van Diephen, *J. Chem. Phys.*, 1969, **50**, 137.
14. I. Umehara, N. Nagai and Y. Ōnuki, *J. Phys. Soc. Jpn.*, 1991, **60**, 1294.
15. I. Umehara, Y. Kurosawa, N. Nagai, M. Kikuchi, K. Satoh and Y. Ōnuki, *J. Phys. Soc. Jpn.*, 1990, **59**, 2848.

16. Y. Onuki and Rikio Settai, *Low Temperature Physics/Fizika Nizkikh Temperatur*, 2012, **38**, 119.
17. N. D. Mathur, F. M. Grosche, S. R. Julian, I. R. Walker, D. M. Freye, R. K. W. Haselwimmer and G. G. Lonzarich, *Nature*, 1998, **394**, 39.
18. Z. Kletowski, *Solid State Commun.*, 1987, **62**, 745.
19. K. Kawashima, M. Maruyama, M. Fukuma and J. Akimitsu, *Phys. Rev. B*, 2010, **82**, 094517.
20. A. Freeman and D. Koelling, *Journal de Physique*, 1972, **33**, C3-57.
21. S. D. Johnson, J. R. Young, R. J. Zieve and J. C. Cooley, *Solid State Commun.*, 2012, **152**, 513.
22. W. R. Johanson, G. W. Crabtree, A. S. Edelstein and O. D. MacMasters, *Phys. Rev. Lett.*, 1981, **45**, 504.
23. R. Settai, K. Sugiyama, A. Yamaguchi, S. Araki, K. Miyake, T. Takeuchi, K. Kindo, Y. Onuki and Z. Kletowski, *J. Phys. Soc. Jpn.*, 2000, **69**, 3983.
24. K. A. Jr. Gschneider, S. K. Dhar, R. J. Stierman, T. W. E. Tsang and O. D. MacMasters, *J. Magn. & Magn. Mater.*, 1985, **47 & 48**, 51.
25. A. P. Murani, *Phys. Rev. B*, 1983, **28**, 2308.
26. Y. Onuki and R. Settai, *Low Temp. Phys.*, 2012, **38**, 89.
27. T. Iizuka, T. Mizuno, B. Hun Min, Y. S. Kwon and S. ichi Kimura, *J. Phys. Soc. Jpn.*, 2012, **81**, 043703.
28. J. A. Abraham, G. Pagare, S. S. Chouhan and S. P. Sanyal, *Comput. Mater. Sci.*, 2014, **81**, 423.
29. J. A. Abraham, G. Pagare, S. S. Chouhan and S. P. Sanyal, *Intermetallics*, 2014, **51**, 1.

30. P. Blaha, K. Schwarz, G.k.H. Madsen, D. Kuasnicka and J. Luitz, WIEN2K, an augmented plane wave+local orbitals program for calculating crystal properties, K. Schwarz Technical Universitat, Wien, Austria, 2001.
31. O. K. Andersen, *Phys. Rev. B*, 1975, **12**, 3060.
32. J. P. Perdew and A. Zunger, *Phys. Rev. B*, 1981, **23**, 5048.
33. J. P. Perdew, K. Burke and M. Ernzerhop, *Phys. Rev. Lett.*, 1996, **77**, 3865.
34. J. P. Perdrew, A. Ruzsinszky, G. I. Csonka, O. A. Vydrov, G. E. Scuseria, L. A. Constantin, X. Zhou, K. Burke, *Phys. Rev. Lett.*, 2008, **100**, 136406.
35. Z. Wu and R.E. Cohen, *Phys. Rev. B*, 2006, **73**, 235116.
36. A. D. Becke, *J. Chem. Phys.*, 1993, **98**, 5648.
37. J. P. Perdew, S. Kurth, A. Zupan, P. Blaha, *Phys. Rev. Lett.*, 1999, **82**, 2544.
38. Z. Ali, B. Khan, I. Ahmad, I. Khan, S. Jalali Asadabadi, *Journal of J. Magn. Magn. Mater.*, 2015, **381**, 34.
39. S. Jalali, Asadabadi, *Phys. Rev. B*, 2007, **75**, 205130.
40. S. Jalali Asadabadi and F. Kheradmand, *J. Appl. Phys.*, 2010, **108**, 073531.
41. V. I. Anisimov, I. V. Solovyev, M. A. Korotin, M. T. Czyzyk and G. A. Sawatzky, *Phys. Rev. B*, 1993, **48**, 16929.
42. D. D. Koelling and B. N. Harmon, *J. Phys. C*, 1977, **10**, 3107.
43. P. Novak, "Calculation of spin-orbit coupling" 1997, http://www.wien2k.a/reg_user/textbooks/novak_lecture_on_spinorbit.ps.
44. H. J. Monkhorst and J. D. Pack, *Phys. Rev. B*, 1976, **13**, 5188.
45. M. Jamal, S. J. Asadabadi, I. Ahmad and H. A. R. Aliabad, *Comp. Mater. Sci.*, 2014, **95**, 592.

46. R. Stadler, W. Wolf, R. Podloucky, G. Kresse, J. Furthmuller and J. Hafner, *Phys. Rev. B*, 1996, **54**, 1729.
47. M. Shafiq, S. Arif, I. Ahmad, S. Jalali Asadabadi, M. Maqbool and H. A. R. Aliabad, *J. Alloys Compd.*, 2015, **618**, 292.
48. M. Shafiq, I. Ahmad and S. J. Asadabadi, *J. Appl. Phys.*, 2014, **116**, 103905.
49. F. Birch, *Phys. Rev.* 1947, **71**, 809.
50. K. A. Jr. Gschneidner, M. Ji, C. Z. Wang, K. M. Hoa, A. M. Russell, Ya. Mudryk, A. T. Becker and J. L. Larson, *Acta Materialia*, 2009, **57**, 5876.
51. M. Zarshenas and S. J. Asadabadi, *Thin Solid Film*, 2012, **520**, 2901.
52. K. Tao, J. Zhou, Q. Sun, Q. Wang, V. S. Stepanyuk and P. Jena, *Phys. Rev. B*, 2014, **89**, 085103.
53. H. Onishi, *J. Phys.: Conference Series* 2012, **391**, 012102.
54. S. B. Dugdale, *Phys. Rev. B*, 2011, **83**, 012502.
55. C. Stassis, J. Zarestky, C. K. Loong, O. D. McMasters and R. M. Nicklow, *Phys. Rev. B*, 1981, **23**, 2227.
56. M. Born and K. Huang, *Dynamical Theory of Crystal Lattices* (Clarendon, Oxford, 1954).
57. R. Hill, *Proc. Phys. Soc. London*, 1952, **65**, 350.
58. A. Reuss and *Z. Angew. Math. Mech.*, 1929, **9**, 49.
59. W. Voigt, *Lehrbuch der Kristallphysik* (Teubner, Leipzig, 1928).
60. S. F. Pugh, *Philos. Mag.*, 1954, **45**, 823.
61. V. Kanchana, *EPL*, 2009, **87**, 26006.
62. H. Fu, D. Li, F. Peng, T. Gao and X. Cheng, *Comput. Matter. Sci.*, 2008, **44**, 774.

63. L. Kleinman, Phys. Rev. 1962, **128**, 2614.
64. V. Tvergaard and J. W. Hutchinson, J. Am. Ceram. Soc., 1988, **71**, 157.
65. L. Fast, J. M. Wills, B. Johansson and O. Eriksson, Phys. Rev. B, 1995, **51**, 17431.
66. J. P. Sanchez, J. M. Friedt, G. K. Shenoy, A. Percheron, and J. C. Achard, J. Phys. C: Solid State Phys., 1976, **9**, 2207.